Published in final edited form as:
Chem Res Toxicol. 2009 June ; 22(6): 1189–1193. doi:10.1021/tx900107q.

Absolute Configurations of Spiroiminodihydantoin and Allantoin Stereoisomers: Comparison of Computed and Measured Electronic Circular Dichroism Spectra

Shuang Ding[†], **Lei Jia**[†], **Alexander Durandin**[‡], **Conor Crean**[‡], **Alexander Kolbanovskiy**[‡], **Vladimir Shafirovich**[‡], **Suse Broyde**[†], and **Nicholas E. Geacintov**[*,‡]

[†]Department of Biology, New York University, New York, NY 10003

[‡]Department of Chemistry, New York University, New York, NY 10003

Abstract

The assignment of absolute configurations is of critical importance for understanding the biochemical processing of DNA lesions. The diastereomeric spiroiminodihydantoin (Sp) lesions are oxidation products of guanine and 8-oxo-7,8-dihydroguanine (8-oxoG), and the absolute configurations of the two diastereomers, Sp1 and Sp2, have been evaluated by experimental and computational optical rotatory dispersion (ORD) methods. In order to support our previous assignments by the ORD method, we calculate the electronic circular dichroism spectra (ECD) of the Sp stereoisomers. Comparison of the experimentally measured and computed ECD spectra indicates that Sp1 has (−)-*S* absolute configuration, while Sp2 has (+)-*R* absolute configuration. Thus, the *S* and *R* assignments, based on the ECD spectra of Sp1 and Sp2, are consistent with our previous assignments of absolute configurations. To further test the validity of this approach, we performed a proof-of-principle computation of the ECD and ORD of the *R* and *S* enantiomers of allantoin (similar in chemical composition to Sp) of known absolute configurations. The calculations provide the correct assignment of the absolute configurations of the allantoin enantiomers, indicating that the computational TDDFT approach is robust for identifying the absolute configurations of allantoins, and probably the Sp stereoisomers, as has been shown previously for other organic molecules.

Introduction

The recent development of improved computational methods based on time-dependent density functional theory (TDDFT) for calculating optical rotatory dispersion (ORD) and electronic circular dichroism (ECD) spectra has increased the reliability of determining the absolute configurations of chiral organic molecules (1-3). The combined use of both the ORD and ECD characteristics leads to more robust assignments of absolute configurations (4) and provides reasonable agreement between computed and experimentally measured ORD and ECD spectra (3, 5-7). Recently, we determined the absolute configurations of the

[*]Corresponding author: Tel: 212-998-8407, Fax: 212-998-8421, ng1@nyu.edu.

Supporting Information Available: Figure S1: CD spectra of Sp1 and Sp2 in acetonitrile; Figure S2: ORD spectrum of Sp1 in acetonitrile. This material is available free of charge via the Internet at http://pubs.acs.org.

two spiroiminodihydantoin (Sp) nucleobase stereoisomers Sp1 and Sp2 that are well known oxidation products of guanine and 8-oxo-7,8-dihydroguanine in DNA (8-11). These two nucleoside stereoisomers are distinguishable according to their elution order in reversed phase HPLC experiments using Hypercarb columns since dSp1 (the 2′-deoxyribonucleoside) elutes before dSp2 (12). However, this order of elution is reversed when a normal-phase amino Hypersil column is utilized as reported by Ravanat and Cadet (13). We confirmed this difference by performing HPLC experiments with both types of columns by comparing the shapes and signs of the CD spectra with those of Ravanat and Cadet (their NH_2-Hypersil elution products 2 and 3 have the same spectral characteristics as our Hypercarb elution products dSp2 and dSp1, respectively). As noted previously (12), the CD spectra of the individual precursor dSp1 and dSp2 nucleosides are very similar in sign and wavelength dependence to the Sp1 and Sp2 spectra, respectively.

The assignment of absolute configuration is of critical importance for understanding the biochemical processing of these unusual, propeller-like lesions (14-19). Experimental (20) and computational (21) studies have shown that the absolute configurations of the two Sp lesions severely distort the DNA duplex in a stereoisomer-dependent manner. Both are highly mutagenic, causing G -> C and G -> T transversion mutations in *E. coli* (15, 16, 22). It has been observed that the mutational properties of these lesions in *E. coli* are stereochemistry-dependent (15). The Sp1 and Sp2 lesions are also repaired with different efficiencies via the base excision repair pathway by the human Neil1 glycosylase (23).

In order to determine the absolute configurations of Sp1 and Sp2 nucleobases, we previously measured and reported the ORD spectra of each enantiomer, and computed the ORD values by TDDFT methods. These computations were based on quantum mechanically geometry-optimized structures of each enantiomer (Figure 1), whose *R* and *S* designations for the chiral centers of these amino tautomers follow the standard IUPAC convention (24, 25). We then compared the signs and wavelength dependence of the computed and measured ORD spectra for each enantiomer in the ~ 280 – 600 nm wavelength region. While there are well-known limitations in the accuracy of the ORD computations (26), the shapes and signs of the computed and observed ORD spectra matched reasonably well (12). A comparison of the measured and computed signs of the wavelength-dependent ORD values provided the key to assigning the absolute configurations of the Sp1 and Sp2 enantiomers. On the basis of these results, we concluded that the Sp1 enantiomer has (−)-*S*, while Sp2 has (+)-*R* absolute configuration. Recently, Karwowski et al. described the assignment of the absolute configurations of the Sp stereoisomers by an approach based on the interactions between protons of the modified base and the sugar moieties in dimethylsulfoxide solution using one- and two-dimensional NMR methods, combined with molecular modeling and quantum mechanical calculations (27). However, based on a detailed analysis of the NMR data, these authors concluded that the absolute configurations of Sp1 and Sp2 are *R* and *S*, respectively, which is opposite to our findings based on ORD measurements (12).

Here, we calculate the electronic circular dichroism spectra of the spiroiminodihydantoin stereoisomers in order to substantiate our previous assignments by the ORD method. The computed ECD spectra are then compared to the experimentally measured ECD spectra (12). The characteristic wavelength dependence in the ECD spectra of the two dSp

stereoisomers is more easily measured than the ORD spectra, thus providing a more convenient approach for their identification.

The TDDFT method has recently been employed to compute both ORD values and ECD spectra (7). Predictions of the optical rotations and ECD using DFT methods have been successfully correlated with experimental data for a variety of chiral molecules (3, 5, 7). When convergent results are obtained by both methods, the assignment of absolute configuration is considered to be more reliable than assignments based on only one of these optical spectroscopic methods alone (1, 3, 4).

In the absence of a crystal structure for Sp that could have unambiguously validated the results derived from either the ORD/TDDFT calculations (12) or the NMR results (27), we also performed a proof-of-principle computation of the ECD and ORD of the *R* and *S* enantiomers of allantoin (Figure 1). Allantoin is similar in chemical composition to spiroiminodihydantoin (Figure 1) and is derived from the oxidation of uric acid. A crystal structure of the naturally occurring *S* enantiomer is available (28) (PDB ID 2q37). This crystal structure served as the basis for generating the coordinates of the *R* mirror image allantoin enantiomer in our computations (see Methods). The computed and observed ECDs of the *R* and *S* allantoin enantiomers have similar shapes and signs as the *R* and *S* mirror image ECD spectra. These findings further support the value of the ECD calculations as a reliable tool for the assignment of absolute configuration in cases of small molecules such as the stereoisomeric guanine oxidation products allantoin and Sp.

Methods

The calculations of ECD of Sp1 and Sp2 were carried out by TDDFT methods with Gaussian 03 (29). The QM-optimized geometry of the Sp *R* and *S* enantiomers had been previously obtained by DFT methods at the B3LYP/6-31G(d) level (30). The excitation energies and rotational strengths were calculated using TDDFT at the B3LYP/6-311++G(2d, 2p) level, as in the ORD calculations. The ECD spectrum is simulated from electronic excitation energies and velocity rotational strengths by overlapping the Gaussian function for each transition (6, 31). For the parameter σ (width of the band at 1/e height), a value of 0.15 eV was selected to give a good fit to the experimental spectra.

The same methods were utilized to compute ECD of the *S* and *R* enantiomers of allantoin. A crystal structure of *S*-allantoin (28) (PDB ID 2q37) provided the coordinates for this case. The *R* enantiomer coordinates were generated by inverting the signs of the x coordinates, a standard transformation procedure for generating the coordinates of one enantiomer from its mirror image. In this case, a value of 0.25 eV was selected for the parameter σ.

Results and Discussion

The calculated ECD, based on the quantum mechanically optimized geometries of the *R* and *S* Sp stereoisomers, resemble the experimentally measured spectra in shape and sign (Figure 2). The simulated spectra exhibit three CD bands in the 180 – 340 nm range (Figure 2A) that resemble the experimental bands in sign, shape, and relative magnitude, with the longest wavelength bands exhibiting the smallest amplitudes in both cases (Figure 2B). However,

the calculated ECD bands are generally blue-shifted by about 10-20 nm relative to the experimentally measured CD bands. These differences are most likely due to imperfections in the density functional and the neglect of solvent and vibrational effects (32).

Comparison of the experimentally measured and computed ECD spectra, together with the signs of the ORD values in the visible region of the spectrum (12), clearly indicate that Sp1 has (−)-*S* absolute configuration, while Sp2 has (+)-*R* absolute configuration. Thus, the *S* and *R* assignments, based on the circular dichroism spectra of Sp1 and Sp2, are completely consistent with our previous assignments of absolute configurations on the basis of the computed and experimentally measured ORD spectra alone (12).

The available X–ray crystallographic structure of the (+)*S* allantoin enantiomer, together with published ECD spectra (28, 33, 34) of either one or the other, or both allantoin enantiomers, together with published ORD spectra of the (−)*R* allantoin enantiomer (33), provide an opportunity for testing the ability of the computational DFT methods to accurately predict the absolute configuration of the two allantoin enantiomers of known absolute configurations. The computed and experimentally measured ECD spectra calculated for the *R* and *S* allantoin enantiomers are shown in Figure 3, while the calculated ORD spectra are shown in Figure 4. The calculated long wavelength ORD values are positive for *S*-allantoin and negative for *R*-allantoin, in agreement with the experimentally measured long-wavelength ORD part of the spectrum of the (−)*R* allantoin enantiomer (33). The signs and shapes of the computed and experimental ECD spectra are in agreement with one another, although the computed maxima and minima are blue-shifted by ~ 10 – 20 nm, relative to the experimentally measured ECD spectra (28, 33, 34), just as in the case of the computed Sp ECD spectra. Besides the reasons already mentioned for the differences between the calculated and experimental ECD spectra, there are other reasons as well in the case of the allantoin enantiomers. First, because of the ring-opened character of allantoin, the structures may be conformationally flexible according to computed results (35), and thus multiple conformations may affect the computed and experimental ECD values and spectra. We utilized a structure observed crystallographically (28) in our computations. In addition, both the ORD and ECD spectra vary as a function of pH and this effect may account for some of the more subtle differences in the shapes of the published CD spectra of the allantoin stereoisomers (28, 33, 34). It is possible that different conformers or perhaps even different tautomers with different conformations arise when the solution pH is varied. However, a further exploration of these issues was beyond the scope of the present study.

The ECD spectra of both allantoin enantiomers published recently by Rammazina et al. (34) are replotted in Figure 3B. The ratios of the magnitudes of the shorter wavelength ECD band to the magnitude of the longer ECD wavelength band is > 10, whereas smaller values of this ratio have been published for the (−)*R* (33) and the (+)*S* (28) enantiomers (~ 5 and ~ 2, respectively). Our computed ratios are closer to these latter values. Overall, the computed ECD spectra and the long-wavelength ORD spectra provide the correct assignments of the absolute configurations of the allantoin enantiomers that have been validated by X-ray crystallographic methods (28).

Finally, the identification of stereoisomeric spiroiminodihydantoin lesions embedded in oligonucleotides may not be feasible using direct measurements of the cicular dichroism spectra of the modified oligonucleotides. The DNA and spiroiminodihydantoin ECD spectra overlap in the UV region below 300 nm. In such cases it is necessary to enzymatically digest the oligonucleotides and isolate the dSp stereoisomers so that these modified 2′-deoxynucleosides can be each identified via their characteristic ECD spectra as shown in Figure 2B.

The possibility exists that different Sp tautomers may occur in non-protic organic solvents, and that there may be significant differences in the ORD and ECD spectra measured in aqueous solution and in organic solvents. We have therefore measured the ECD spectra of the two Sp stereoisomers in the polar organic solvent acetonitrile (Figure S1, Supporting Information), and these spectra are almost identical to the ECD spectra of the same stereoisomers in aqueous solution (Figure 2B). Furthermore, the sign of the ORD signal of Sp1 is the same in acetonitrile and water (Figure S2, Supporting Information). Since the ECD characteristics of the spiroiminodihydantoin stereoisomers are indistinguishable in aqueous and acetonitrile solutions, we conclude that the assignments of the absolute configurations in aqueous solution are not affected significantly by solvent and probably tautomerization, a topic that we have also addressed earlier (12).

Conclusions

Because the ECD and ORD signals are interdependent and coupled by the Kronig-Kramer relationship (36), either method is sufficient for comparing computed and experimental ECD or ORD spectra. Since opposite assignments have been obtained by an analysis of NMR spectra of the nucleosides of dSp1 and dSp2 in dimethyl sulfoxide solution (27), this discrepancy must await further resolution. Nevertheless, the correct assignment of the absolute configurations of the allantoin enantiomers based on computed ECD and ORD spectra, suggests that the computational TDDFT approach is robust for identifying the absolute configurations of allantoin, as has already been shown for other organic molecules (3, 5-7).

Supplementary Material

Refer to Web version on PubMed Central for supplementary material.

Acknowledgments

We would like to thank Dr. C. Burrows for suggesting the allantoin TDDFT/ECD/ORD calculations. We would like to thank Drs. C. Percudani and I. Ramazzina for directing us toward their experimental publication (34) containing the ECD data for allantoin *S* and *R* stereoisomers. This work was supported, in part, by NIH Grant 1R01 ES11589 (V.S.), and by NIH 2R01 CA75449 (S.B.). Partial support for computational infrastructure and systems management was also provided by Grant CA-28038 (S.B.). Components of this work were conducted in a Shared Instrumentation Facility constructed with support from Research Facilities Improvement Grant C06 RR-16572 from the National Center for Research Resources, NIH. The content is solely the responsibility of the authors and does not necessarily represent the official views of the National Cancer Institute or the National Institutes of Health.

References

(1). Petrovic AG, Polavarapu PL. Chiroptical spectroscopic determination of molecular structures of chiral sulfinamides: t-butanesulfinamide. J. Phys. Chem. A. 2007; 111:10938–10943. [PubMed: 17924612]

(2). Petrovic AG, Vick SE, Polavarapu PL. Determination of the absolute stereochemistry of chiral biphenanthryls in solution phase using chiroptical spectroscopic methods: 2,2′-Diphenyl-[3,3′-biphenanthrene]-4,4′-diol. Chirality. 2008; 20:501–510. [PubMed: 17963199]

(3). Stephens PJ, McCann DM, Devlin FJ, Cheeseman JR, Frisch MJ. Determination of the absolute configuration of [3(2)](1,4)barrelenophanedicarbonitrile using concerted time-dependent density functional theory calculations of optical rotation and electronic circular dichroism. J. Am. Chem. Soc. 2004; 126:7514–7521. [PubMed: 15198598]

(4). Polavarapu PL. Why is it important to simultaneously use more than one chiroptical spectroscopic method for determining the structures of chiral molecules? Chirality. 2008; 20:664–672. [PubMed: 17924421]

(5). Kwit M, Sharma ND, Boyd DR, Gawronski J. Absolute configuration of conformationally flexible cis-dihydrodiol metabolites by the method of confrontation of experimental and calculated electronic CD spectra and optical rotations. Chem. Eur. J. 2007; 13:5812–5821. [PubMed: 17397025]

(6). Giorgio E, Tanaka K, Verotta L, Nakanishi K, Berova N, Rosini C. Determination of the absolute configurations of flexible molecules: Synthesis and theoretical simulation of electronic circular dichroism/optical rotation of some pyrrolo[2,3-b]indoline alkaloids - A case study. Chirality. 2007; 19:434–445. [PubMed: 17393468]

(7). Stephens PJ, McCann DM, Butkus E, Stoncius S, Cheeseman JR, Frisch MJ. Determination of absolute configuration using concerted ab Initio DFT calculations of electronic circular dichroism and optical rotation: bicyclo[3.3.1]nonane diones. J. Org. Chem. 2004; 69:1948–1958. [PubMed: 15058939]

(8). Luo W, Muller JG, Rachlin EM, Burrows CJ. Characterization of spiroiminodihydantoin as a product of one-electron oxidation of 8-Oxo-7,8-dihydroguanosine. Org. Lett. 2000; 2:613–616. [PubMed: 10814391]

(9). Suzuki T, Masuda M, Friesen MD, Ohshima H. Formation of spiroiminodihydantoin nucleoside by reaction of 8-oxo-7,8-dihydro-2′-deoxyguanosine with hypochlorous acid or a myeloperoxidase-H_2O_2-Cl^- system. Chem. Res. Toxicol. 2001; 14:1163–1169. [PubMed: 11559029]

(10). Adam W, Arnold MA, Grune M, Nau WM, Pischel U, Saha-Möller CR. Spiroiminodihydantoin is a major product in the photooxidation of 2′-deoxyguanosine by the triplet states and oxyl radicals generated from hydroxyacetophenone photolysis and dioxetane thermolysis. Org. Lett. 2002; 4:537–540. [PubMed: 11843585]

(11). Cadet J, Douki T, Ravanat JL. Oxidatively generated damage to the guanine moiety of DNA: mechanistic aspects and formation in cells. Acc. Chem. Res. 2008; 41:1075–1083. [PubMed: 18666785]

(12). Durandin A, Jia L, Crean C, Kolbanovskiy A, Ding S, Shafirovich V, Broyde S, Geacintov NE. Assignment of absolute configurations of the enantiomeric spiroiminodihydantoin nucleobases by experimental and computational optical rotatory dispersion methods. Chem. Res. Toxicol. 2006; 19:908–913. [PubMed: 16841958]

(13). Ravanat JL, Cadet J. Reaction of singlet oxygen with 2′-deoxyguanosine and DNA. Isolation and characterization of the main oxidation products. Chem. Res. Toxicol. 1995; 8:379–388. [PubMed: 7578924]

(14). Henderson PT, Delaney JC, Gu F, Tannenbaum SR, Essigmann JM. Oxidation of 7,8-dihydro-8-oxoguanine affords lesions that are potent sources of replication errors in vivo. Biochemistry. 2002; 41:914–921. [PubMed: 11790114]

(15). Henderson PT, Delaney JC, Muller JG, Neeley WL, Tannenbaum SR, Burrows CJ, Essigmann JM. The hydantoin lesions formed from oxidation of 7,8-dihydro-8-oxoguanine are potent sources of replication errors in vivo. Biochemistry. 2003; 42:9257–9262. [PubMed: 12899611]

(16). Kornyushyna O, Berges AM, Muller JG, Burrows CJ. In vitro nucleotide misinsertion opposite the oxidized guanosine lesions spiroiminodihydantoin and guanidinohydantoin and DNA synthesis past the lesions using Escherichia coli DNA polymerase I (Klenow fragment). Biochemistry. 2002; 41:15304–15314. [PubMed: 12484769]

(17). Kornyushyna O, B. CJ. Effect of the oxidized guanosine lesions spiroiminodihydantoin and guanidinohydantoin on proofreading by escherichia coli DNA Polymerase I (Klenow Fragment) in different sequence contexts. Biochemistry. 2003; 42:13008–13018. [PubMed: 14596616]

(18). Hailer MK, Slade PG, Martin BD, Rosenquist TA, Sugden KD. Recognition of the oxidized lesions spiroiminodihydantoin and guanidinohydantoin in DNA by the mammalian base excision repair glycosylases NEIL1 and NEIL2. DNA Repair. 2005; 4:41–50. [PubMed: 15533836]

(19). Hailer MK, Slade PG, Martin BD, Sugden KD. Nei deficient Escherichia coli are sensitive to chromate and accumulate the oxidized guanine lesion spiroiminodihydantoin. Chem. Res. Toxicol. 2005; 18:1378–1383. [PubMed: 16167829]

(20). Chinyengetere F, Jamieson ER. Impact of the oxidized guanine lesion spiroiminodihydantoin on the conformation and thermodynamic stability of a 15-mer DNA duplex. Biochemistry. 2008; 47:2584–2591. [PubMed: 18281959]

(21). Jia L, Shafirovich V, Shapiro R, Geacintov NE, Broyde S. Structural and thermodynamic features of spiroiminodihydantoin damaged DNA duplexes. Biochemistry. 2005; 44:13342–13353. [PubMed: 16201759]

(22). Neeley WL, Delaney S, Alekseyev YO, Jarosz DF, Delaney JC, Walker GC, Essigmann JM. DNA polymerase V allows bypass of toxic guanine oxidation products in vivo. J. Biol. Chem. 2007; 282:12741–12748. [PubMed: 17322566]

(23). Krishnamurthy N, Zhao XB, Burrows CJ, David SS. Superior removal of hydantoin lesions relative to other oxidized bases by the human DNA glycosylase hNEIL1. Biochemistry. 2008; 47:7137–7146. [PubMed: 18543945]

(24). Prelog V, Helmchen G. Basic principles of the CIP-system and proposals for a revision. Angew. Chem. Int. Ed. Engl. 1982; 21:567–583.

(25). Cahn RS, Ingold C, Prelog V. Specification of molecular chirality. Angew. Chem. Int. Ed. 1966; 5:385–415.

(26). Stephens PJ, Devlin FJ, Cheeseman JR, Frisch MJ, Bortolini O, Besse P. Determination of absolute configuration using ab initio calculation of optical rotation. Chirality. 2003; 15:S57–S64. [PubMed: 12884375]

(27). Karwowski B, Dupeyrat F, Bardet M, Ravanat JL, Krajewski P, Cadet J. Nuclear magnetic resonance studies of the 4R and 4S diastereomers of spiroiminodihydantoin 2′-deoxyribonucleosides: absolute configuration and conformational features. Chem. Res. Toxicol. 2006; 19:1357–1365. [PubMed: 17040105]

(28). Kim K, Park J, Rhee S. Structural and functional basis for (S)-allantoin formation in the ureide pathway. J. Biol. Chem. 2007; 282:23457–23464. [PubMed: 17567580]

(29). Frisch, MJ.; Trucks, GW.; Schlegel, HB.; Scuseria, GE.; Robb, MA.; Cheeseman, JR.; Montgomery, JJA.; Vreven, T.; Kudin, KN.; Burant, JC.; Millam, JM.; Iyengar, SS.; Tomasi, J.; Barone, V.; Mennucci, B.; Cossi, M.; Scalmani, G.; Rega, N.; Petersson, GA.; Nakatsuji, H.; Hada, M.; Ehara, M.; Toyota, K.; Fukuda, R.; Hasegawa, J.; Ishida, M.; Nakajima, T.; Honda, Y.; Kitao, O.; Nakai, H.; Klene, M.; Li, X.; Knox, JE.; Hratchian, HP.; Cross, JB.; Bakken, V.; Adamo, C.; Jaramillo, J.; Gomperts, R.; Stratmann, RE.; Yazyev, O.; Austin, AJ.; Cammi, R.; Pomelli, C.; Ochterski, JW.; Ayala, PY.; Morokuma, K.; Voth, GA.; Salvador, P.; Dannenberg, JJ.; Zakrzewski, VG.; Dapprich, S.; Daniels, AD.; Strain, MC.; Farkas, O.; Malick, DK.; Rabuck, AD.; Raghavachari, K.; Foresman, JB.; Ortiz, JV.; Cui, Q.; Baboul, AG.; Clifford, S.; Cioslowski, J.; Stefanov, BB.; Liu, G.; Liashenko, A.; Piskorz, P.; Komaromi, I.; Martin, RL.; Fox, DJ.; Keith, T.; Al-Laham, MA.; Peng, CY.; Nanayakkara, A.; Challacombe, M.; Gill, PMW.; Johnson, B.; Chen, W.; Wong, MW.; Gonzalez, C.; Pople, JA. Gaussian, Gaussian, Inc.; Wallingford CT: 2004.

(30). Jia L, Shafirovich V, Shapiro R, Geacintov NE, Broyde S. Spiroiminodihydantoin lesions derived from guanine oxidation: structures, energetics, and functional implications. Biochemistry. 2005; 44:6043–6051. [PubMed: 15835893]

(31). Diedrich C, Grimme S. Systematic investigation of modern quantum chemical methods to predict electronic circular dichroism spectra. J. Phys. Chem. A. 2003; 107:2524–2539.

(32). McCann DM, Stephens PJ. Determination of absolute configuration using density functional theory calculations of optical rotation and electronic circular dichroism: chiral alkenes. J. Org. Chem. 2006; 71:6074–6098. [PubMed: 16872191]

(33). ’s-Gravenmade EJ, Vogels GD, van Pelt C. Preparation, properties and absolute configuration of (−)-allantoin. Recl. Trav. Chim. Pays-Bas. 1969; 88:929–939.

(34). Ramazzina I, Cendron L, Folli C, Berni R, Monteverdi D, Zanotti G, Percudani R. Logical identification of an allantoinase analog (puuE) recruited from polysaccharide deacetylases. J. Biol. Chem. 2008; 283:23295–23304. [PubMed: 18550550]

(35). Kahn K, Tipton PA. Kinetics and mechanism of allantoin racemization. Bioorg. Chem. 2000; 28:62–72.

(36). Djerassi, C. Optical Rotatory Dispersion. McGraw-Hill; New York, NY: 1960.

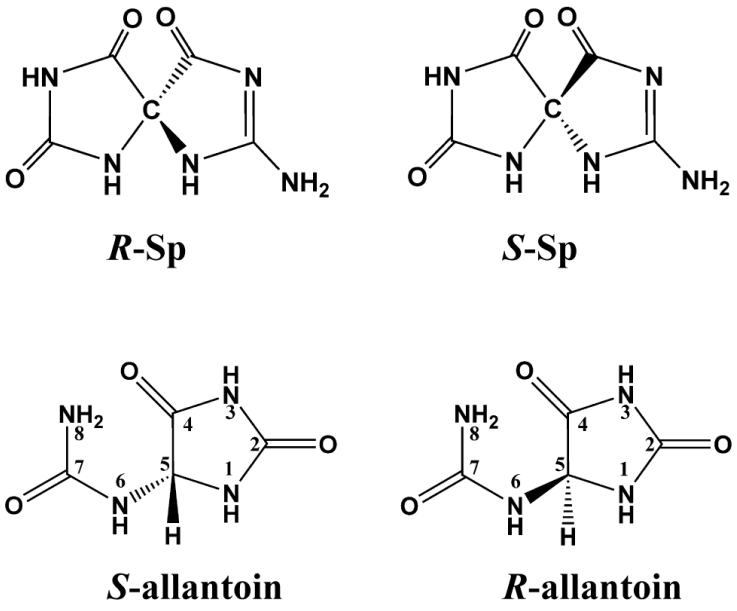

Figure 1.
Chemical structures of Sp nucleobase and allantoin enantiomers.

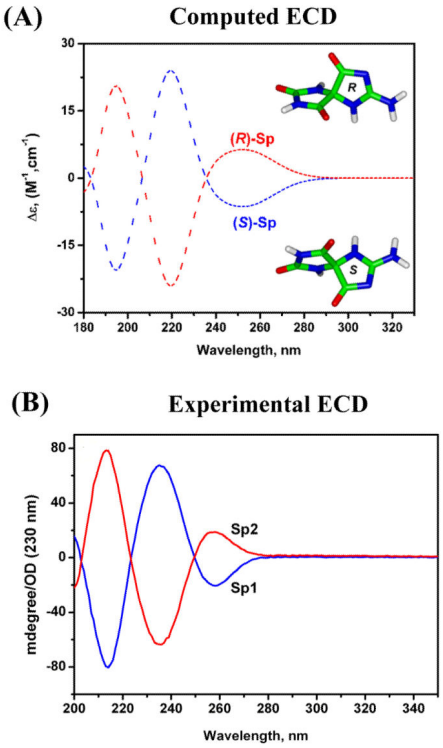

Figure 2.

Comparison of calculated and experimentally measured ECD spectra for Sp. (A) calculated ECD; (B) experimentally measured ECD spectra of Sp1 and Sp2 in water (0.095 mg/mL). The vertical axis is expressed in degrees divided by the absorbance of the sample solutions measured at 230 nm (1 cm path length) (12). Quantum mechanically, geometry-optimized structures for the *R* and *S* Sp nucleobase enantiomers are also shown in (A). The *R* and *S* designations for the chiral centers are based on the standard IUPAC convention (24, 25).

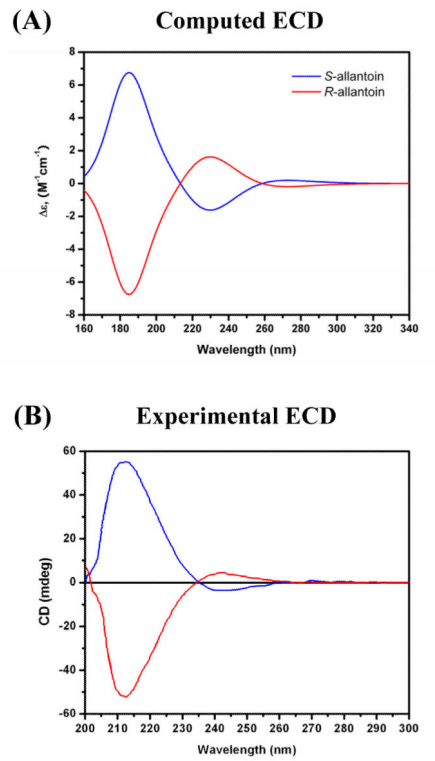

Figure 3.

(A) Calculated ECD of *S* and *R*-allantoin enantiomers (B) Experimental ECD spectra of *S*-allantoin (blue) and *R*-allantoin (red). The experimental ECD spectra were adapted from Figure 2A of Ramazzina et al (34), with the gracious permission of Prof. Riccardo Percudani. These ECD data were obtained using (*S*)-allantoin (0.2 mM) or (*R*,*S*)-allantoin (0.4 mM) as substrates in the presence of PuuE (0.37 μM) in1ml of 0.1 M potassium phosphate, pH 7.6.

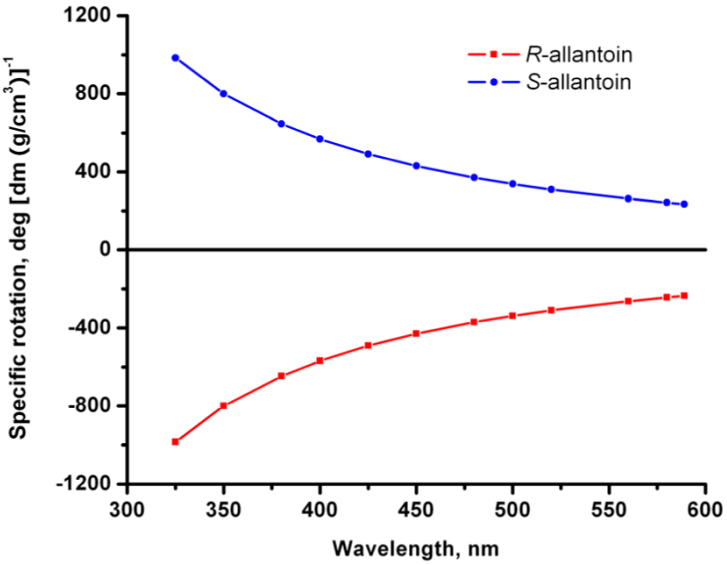

Figure 4.
Calculated ORD of the (+)*S* and (−)*R*-allantoin enantiomers.